

# Anharmonic Phonon Decay in Si Nanowires

Mathieu Luisier

Integrated Systems Laboratory, ETH Zürich, 8092 Zürich, Switzerland, e-mail: mluisier@iis.ee.ethz.ch

**Introduction** The semiconductor industry has recently started to replace the conventional planar Si metal-oxide-semiconductor field-effect transistors (MOSFETs) by three-dimensional FinFET structures with a multi-gate configuration to secure the next 3-4 technology nodes. Looking further into the future of Moore's scaling law, the Fin width and height will have to drastically decrease and go below 5nm to maintain a good electrostatic integrity. The resulting ultra-scaled nanowires (NWs) are expected to play an important role in next generation integrated circuits, both as active components [1-3] as well as energy harvesters through the Seebeck effect [4-5].

The main difference between these two applications resides in their thermal conductivity  $\kappa_{th}$ . While it is important to have a high  $\kappa_{th}$  for transistors so that the heat dissipated during ON-OFF switches can be rapidly evacuated, thermo-generators rely on a low  $\kappa_{th}$  that allows for an efficient conversion of the available heat into energy. A good understanding of the thermal properties of NWs is therefore essential, for both electronic and thermoelectric applications, explaining why nanoscale thermal transport has become a very hot research topic.

Most theoretical investigations of thermal transport through NWs are based either (i) on the Boltzmann Transport Equation, which does not account for phonon quantum confinement [6], (ii) on Molecular Dynamics simulations, which are computationally very intensive and require statistical average over long time periods [7], or (iii) on ballistic phonon Non-equilibrium Green's Function (NEGF) approaches [8]. However, important effects such as the anharmonic decay of high energy phonons into two low energy particles are usually neglected in the NEGF formalism, except for small molecular devices [9-10]. Hence, a NEGF treatment of anharmonic phonon decay in Si NWs is proposed here.

**Simulation Approach** A valence-force-field model with four harmonic interactions is used to model the phonon transport properties at the atomic level [11]. Phonon-phonon scattering takes the form of a self-energy where the anharmonic perturbation potential  $V^{anh}$  contains five cubic interactions as illustrated in Fig. 1 (the  $D$ 's represent phonon Green's Functions,  $dV^{(3)}$  the third derivative of  $V^{anh}$ , and  $E/E'$  phonon energies). Scattering self-energies are introduced in the device contacts too to allow for incoherent phonon injection. A massive parallelization of the workload has been developed to accelerate the simulation time.

**Results** Before simulating Si NWs, the anharmonic phonon decay model was parametrized so that the thermal conductivity of bulk Si could be reasonably-well repro-

duced by the NEGF approach, as shown in Fig. 2. This means that the values of the five parameters  $\alpha$ ,  $\beta$ ,  $\tau$ ,  $\delta_1$ , and  $\delta_3$  in Fig. 1 were tuned to obtain a good match to the experimental data.

Figure 3 demonstrates the importance of injecting phonon into the simulation domain from contacts where phonon-phonon scattering is included. If not, artificial reflections occur at the device boundaries, leading to an unphysical distribution of the phonon population there. Note that for ballistic simulations, in an homogeneous structure, the phonon population is uniformly distributed while there should be more (less) phonons close to the hot (cold) contact, as with anharmonic phonon decay.

Another consequence of phonon-phonon scattering is a decrease of the thermal current  $I_{th}$ , as well as of the thermal conductance  $G_{th}=I_{th}/\Delta T$ , when the NW temperature exceeds 200-250K. This can be observed in Fig. 4. In ballistic simulations,  $I_{th}$  and  $G_{th}$  keeps increasing as function of the temperature so that at 500K, they considerably exceed the more accurate results including anharmonic phonon decay.

Finally, phonon-phonon limited thermal conductivities  $\kappa_{th}$  can be extracted from the simulation results using the  $dR_{th}/dL$  method [12]. The thermal resistance  $R_{th}=1/G_{th}$  is computed for nanowires with different lengths. Due to the diffusive nature of phonon transport,  $R_{th}$  increases linearly as function of the NW length so that a thermal resistivity  $\rho_{th}=dR_{th}/dL$  can be calculated, from which  $\kappa_{th}=1/(\rho_{th}*A)$  is derived ( $A$  is the NW cross section area). The results are shown in Fig. 5: anharmonic phonon decay limits the thermal conductivity of ultra-scaled Si NWs, but less than interface roughness [4].

**Conclusion** A NEGF approach based on an atomistic valence-force-field method and including anharmonic phonon decay has been implemented and used to simulate thermal transport through Si NWs with different transport directions. The results suggest that ballistic simulations greatly overestimate the magnitude of the thermal current flowing through NWs at room temperatures and above. As a next step, anharmonic phonon decay will be combined with interface roughness to study mutual interactions.

**References** [1] Y. Cui et al., Appl. Phys. Lett. **78**, 2214 (2001). [2] A. B. Greytak et al., Appl. Phys. Lett. **84**, 4176 (2004). [3] S. D. Suk et al., IEDM Tech. Dig. **2007**, 891 (2007). [4] A. I. Hochbaum et al., Nature **451**, 163 (2008). [5] A. I. Boukai et al., Nature **451**, 168 (2008). [6] P. Martin et al., Phys. Rev. Lett. **102**, 125503 (2009). [7] D. Donadio et al., Phys. Rev. Lett. **102**, 195901 (2009). [8] T. Markussen et al., Phys. Rev. B **79**, 035415 (2009). [9] N. Mingo, Phys. Rev. B **74**, 125402, (2006). [10] Y. Xu et al., Phys. Rev. B **78**, 224303, (2008). [11] Z. Sui et al., Phys. Rev. B **48**, 17938 (1993). [12] K. Rim et al., IEDM Tech. Dig. **2002**, 4346 (2002).

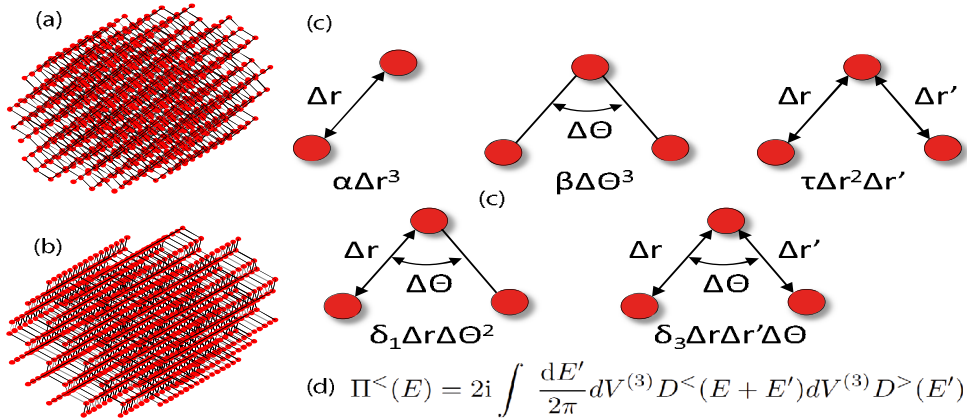


Fig. 1. (a) Schematic view of an ultra-scaled Si nanowire with transport along the  $\langle 100 \rangle$  crystal axis ( $x$ -axis). (b) Same as in (a), but for transport along the  $\langle 110 \rangle$  axis. (c) Schematic representation of the cubic interactions included in the anharmonic perturbation potential  $V^{anh}$  [11]. (d) Lesser scattering self-energy describing anharmonic phonon decay and including all the interactions in (c).

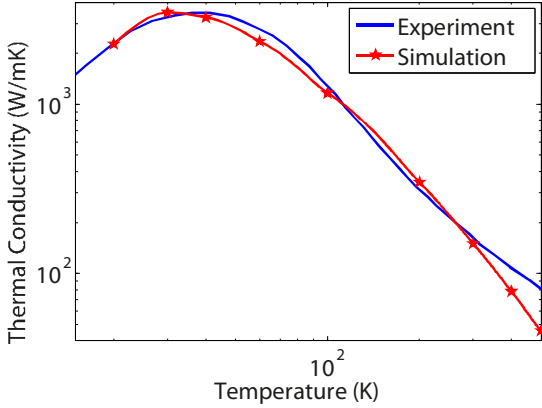


Fig. 2. Simulated (red curve with stars) and measured (blue curve) thermal conductivity  $\kappa_{th}$  of bulk Si as function of the temperature. The values of the parameters  $\alpha$ ,  $\beta$ ,  $\tau$ ,  $\delta_1$ , and  $\delta_3$  in Fig. 1 (c) are fitted to best match the available experimental data.

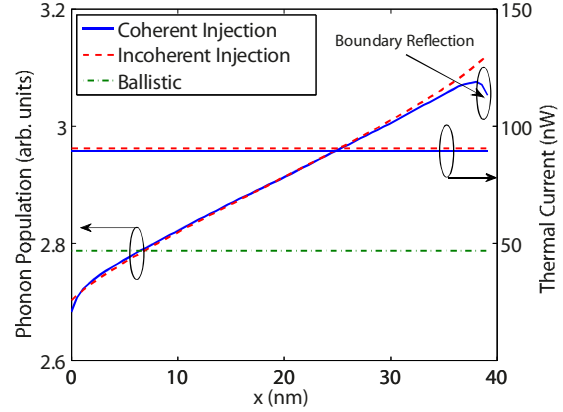


Fig. 3. Phonon population and thermal current along a Si nanowire with a diameter  $d=3\text{nm}$  and a length  $L=40\text{nm}$ . The temperature of the left (right) contact is set to 300K (350K). Coherent (ballistic leads) and incoherent (scattering in the leads) injection mechanisms are compared.

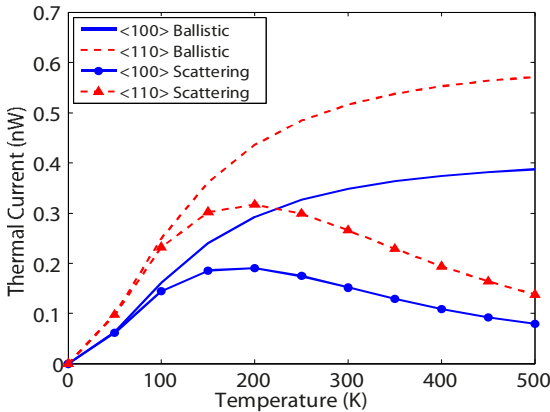


Fig. 4. Thermal current through Si nanowires with a diameter  $d=3\text{nm}$ , a length  $L=60\text{nm}$ ,  $\Delta T=0.1\text{K}$  temperature difference between the contacts, and transport along the  $\langle 100 \rangle$  crystal axis (solid blue lines) and  $\langle 110 \rangle$  (dashed red lines). Results calculated in the ballistic limit of transport (no symbols) and with anharmonic phonon decay (symbols) are shown.

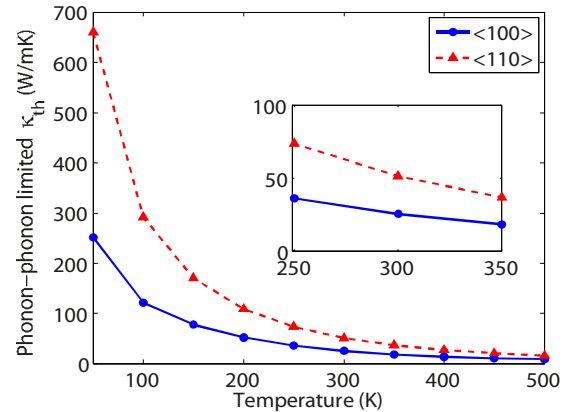


Fig. 5. Anharmonic phonon-phonon limited thermal conductivity  $\kappa_{th}$  of Si nanowires with  $d=3\text{nm}$  and transport along the  $\langle 100 \rangle$  (solid blue line with circles) and  $\langle 110 \rangle$  crystal axis (dashed red line with triangles). The  $dR/dL$  method (derivative of the thermal resistance with respect to the nanowire length) [12] is utilized to compute  $\kappa_{th}$ . Inset:  $\kappa_{th}$  around 300K.